Journal of Water Process Engineering 24 (2018) 49–55

Contents lists available at ScienceDirect

Journal of Water Process Engineering

journal homepage: www.elsevier.com/locate/jwpe

Optimization of solar-driven photo-electro-Fenton process for the treatment of textile industrial wastewater

Edison GilPavas[a,*], Izabela Dobrosz-Gómez[b], Miguel Ángel Gómez-García[c]

[a] GIPAB: Grupo de Investigación en Procesos Ambientales, Departamento de Ingeniería de Procesos, Universidad EAFIT, Cr 49 # 7 Sur 50, Medellín, Colombia
[b] Grupo de Investigación en Procesos Reactivos Intensificados con Separación y Materiales Avanzados – PRISMA, Departamento de Física y Química, Facultad de Ciencias Exactas y Naturales, Universidad Nacional de Colombia, Sede Manizales, Campus La Nubia, km 9 vía Aeropuerto la Nubia, Manizales, Colombia
[c] Grupo de Investigación en Procesos Reactivos Intensificados con Separación y Materiales Avanzados – PRISMA, Departamento de Ingeniería Química, Facultad de Ingeniería y Arquitectura, Universidad Nacional de Colombia, Sede Manizales, Campus La Nubia, km 9 vía Aeropuerto la Nubia, Manizales, Colombia

ARTICLE INFO

Keywords:
Anodic oxidation
Solar Photo-Electro-Fenton
Boron-doped diamond electrode
Industrial wastewater treatment
Solar energy

ABSTRACT

This work deals with the evaluation of a solar-driven Photo Electro-Fenton (SPEF) process as an alternative for the effective degradation of an industrial textile wastewater sample. Experiments were carried out in a laboratory scale batch cell reactor, using boron-doped diamond (anode) and titanium (cathode) electrodes in monopolar configuration. The effect of the main operational parameters (pH, current density (j), conductivity (σ), Fe^{2+} concentration and anode area to effluent volume ((A/V) ratio) on the COD removal and energy consumption were studied using a Box-Behnken experimental design. The SPEF process was optimized using the Response Surface Methodology. At optimum operational conditions (pH = 4, j = 40 mA/cm^2, σ = 5768 μS/cm and Fe^{2+} = 0.3 mM), the solar-driven process achieved total discoloration, COD reduction of 83% and TOC mineralization of 70%, after 15 min of electrolysis. The process yielded a highly oxidized (AOS = 2.24) and biocompatible (BOD_5/COD > 0.4) effluent. Additionally, the most suitable effective surface area of the electrodes (A/V ratio) was determined (3.75 m^{-1}). The analysis of operational costs was also performed. The SPEF process demonstrated to be an efficient alternative for the treatment of industrial wastewater effluent, allowing to achieve Colombian permissible discharge limits.

1. Introduction

The textile industry uses a great amount of chemical compounds (*v.g.*, detergents, waxes, dyes, surfactants, solvents, salts, etc…) and water during its different processes. Consequently, textile wastewater (TWW) is a complex mixture of chemicals characterized with high values of Chemical Oxygen Demand (COD), Total Organic Carbon (TOC) as well as low biodegradability. Indeed, most of TWW is considered as toxic one [1]. In general, TWW is quite difficult to degradate using conventional and/or biological wastewater treatments [2–4]. Thus, the development of new, environmentally friendly technologies, able to reach complete mineralization of pollutants, become an urgent challenge.

Electrochemical oxidation or electro-oxidation (EO) has been recognized as one of the most promising electrochemical procedures for wastewater treatment [5]. The use of simple equipment, easy operation, versatility and environmental compatibility (it does not require the addition of chemicals) are considered as the most important advantages of this technology [6]. In this process, organic matter can be oxidized in two ways: (i) by direct oxidation (anodic oxidation), proceeding on anode surface; and/or (ii) by indirect oxidization (*v.g.*, Electro-Fenton, EF), provoked by electrochemically generated strong oxidants (*v.g.*, hydroxyl radicals: ·OH *via* Fenton's reagent).

In anodic oxidation, ·OH radicals are formed due to water oxidation on a high O_2-overvoltaged anode (reaction (1)).

$$H_2O \rightarrow HO^{\circ}_{Ads} + H^+ + e^- \quad (1)$$

Among the wide variety of available electrodes (anodes) that can be applied in anodic oxidation, the boron-doped diamond (BDD) one stands out due to its following properties: inert surface with low adsorption properties, high resistance to deactivation and to corrosion, high thermal stability, high hardness, good electrical conductivity and an extremely wide potential in aqueous and non-aqueous electrolytes [7].

On the other hand, the EF consists of adding Fenton's reagent to the EO [8]. Thus, the electrogenerated H_2O_2 reacts with Fe^{2+}, present in the medium, leading to the formation of ·OH radicals, as presented in reaction (2).

* Corresponding author.
E-mail address: egil@eafit.edu.co (E. GilPavas).

https://doi.org/10.1016/j.jwpe.2018.05.007
Received 16 January 2018; Received in revised form 5 May 2018; Accepted 13 May 2018

Table 1
Characterization of the industrial TWW together with permissible discharge limits, defined by Colombian legislation, *vs.* characteristics of the obtained effluent after SPEF process.

Parameter	pH	Absorbance (660 nm)	Color (mg Pt-Co/L)	Conductivity (μS/cm)	Turbidity (NTU)	COD (mg O_2/L)	TOC (mg C/L)	BOD_5 (mg O_2/L)	BOD_5/COD ratio	Operating costs, (USD/m^3)
Industrial TWW sample	9.96	1.626	1248	4560	184	545	164	118	0.2165	
Permissible limit[a]	6–9	–		–	–	400	–	200	> 0.4	
SPEF[b] (global efficiency,%)	3.9	0 (100)	51.7 (96)	6280	0 (100)	59.9 (90)	45.9 (79)	35.0 (70)	0.58	1.56

[a] Emission limit values for industrial wastewater discharges into the municipal sewer system, according to Res 0631, 17/03/2015, issued by the Ministry of Environment and Sustainable Development, Colombia.
[b] Optimal operating conditions: pH = 4, j = 40 mA/cm^2, σ = 5768 μS/cm, A/V ratio = 7.5 m^{-1}, Fe^{2+} = 0.3 mM.

$$Fe^{2+} + H_2O_2 \rightarrow Fe^{3+} + HO^{\circ} + OH^{-} \quad (2)$$

The preferred anode for EF is also the BDD one. It presents a remarkable capacity of ·OH radicals production comparing with the other anode materials (*v.g.*, Pt, IrO_2 and PbO_2), allowing the mineralization of organic contaminants in much larger extent [9].

Some drawbacks have to be faced when EO processes are used. Specifically, in the case of EF, its main limitation from the operational point of view, can be the formation of Fe(III)-carboxylate complexes, difficult to destroy by ·OH radicals. It can be solved by subjecting the solution to UV radiation (such process is known as Photo-Electro-Fenton (PEF)). It favors: (i) the enhancement of Fe^{2+} regeneration and ·OH production by photoreduction of $Fe(OH)^{2+}$, Eq. (3); and (ii) the photodecarboxylation of Fe(III)–carboxylate intermediates, Eq. (4) [10–12].

$$Fe(OH)^{2+} + h\nu \rightarrow Fe^{2+} + HO^{\circ} \quad \text{atpH}\sim 3.0 \quad (3)$$

$$Fe(OOCR)^{2+} + h\nu \rightarrow Fe^{2+} + CO_2 + R^{\circ} \quad (4)$$

Moreover, from an economical point of view, an important constraint against the application of EO processes is their high-energy costs associated with the use of artificial light/UV irradiating source. A possible solution for this restriction is the application of direct solar UV. This process is known as Solar Photo-Electro-Fenton (SPEF). Solar-based systems have become an alternative to reduce fossil consumption and greenhouse gas emissions [13,14]. Certainly, solar energy is the most abundant, inexhaustible and clean of all existing energy resources [15,16]. One of the most widespread and studied applications of solar energy is for photovoltaic (PV) power generation [17,18]. It can provide energetic autonomy for solar-driven EO processes since it does not require any connection to the grid.

As far as we know, only few papers presented the applicability of EF and SPEF processes for dyes removal from industrial wastewater [6,9–12]. Among them, it has been reported: (i) direct electrolysis using active electrodes (*v.g.*, TiO_2/RuO_2, reaching 80% of COD and 95% of color removals, after 6 h of treatment) or non-active electrodes (*v.g.*, Nb/BDD anode: 99% of COD removal; SnO_2 electrode: 70% of COD removal after 2 h; PbO_2 electrode: 65% of COD removal) and (ii) heterogeneous photo-electrocatalysis technologies (*v.g.*, TiO_2 electrode, 1 mA cm^{-2}, irradiation time of 1 h with a UV lamp of 21 W cm^{-2}: letting 25% of TOC removal). In these works, synergistic effects due to the combination of the photo irradiation and the electrochemical processes yielded higher removal percentages than these expected basing on the separate contribution of each of oxidation technologies.

This work deals with the evaluation of the SPEF process and its optimization as an alternative for the effective degradation of an industrial TWW sample, not amenable to biodegradation. Experiments were carried out in a laboratory scale batch cell reactor, using BDD (anode) and titanium (cathode) electrodes in monopolar configuration. The effect of the main operational parameters (current density, pH, Fe^{2+} concentration, conductivity, and anode area to effluent volume ratio) on COD removal, TOC mineralization and energy consumption were studied. The solar treatment systems were optimized using the Response Surface Methodology (RSM) [19–23]. A kinetic analysis allowed determination of the time required to meet Colombian permissible discharge limits. The analysis of operational costs was also performed.

2. Materials and methods

2.1. Industrial wastewater samples

TWW samples were collected directly from an equalization tank of an industrial textile plant located in Medellín (Colombia). Before analysis and treatment in the laboratory, samples were kept refrigerated to avoid compounds degradation during storage and transportation, following standard procedures [24]. Table 1 presents their main characteristics. Notice that the wastewaterś COD value was higher than the permissible discharge limits in Colombia, implying the presence of large amount of organic matter. In addition, it was characterized colored effluent with high conductivity value due to high salts concentration. Finally, its initial BOD_5/COD ratio suggested that the analyzed effluent was not amenable to biodegradation [25,26].

2.2. Reactants & analytical methods

All reagents were obtained from Merck and used as received without any further purification: ferrous sulfate hepta-hydrate ($FeSO_4{\cdot}7H_2O$, 99.98%, used as SPEF reagent), H_2SO_4 (99.1%, to adjust sampleś pH), MnO_2 (reagent grade, ≥90%). All solutions were prepared using ultra-pure water (Milli-Q system; conductivity < 1 μS cm^{-1}).

Samples, industrial and these resulting from laboratory tests, were analyzed by triplicate using a UV–VIS double-beam spectrophotometer (Spectronic Genesys 2PC), in the range of 200–700 nm, with a 1 cm path length quartz cell. Standard methods (SM) were used for the quantitative analysis of: COD (the closed reflux method with colorimetric determination, SM-5220D), Total Organic Carbon (TOC, SM-5310D), BOD_5 (the respirometric method, SM-5210B) and turbidity (SM-2130B) [24]. H_2O_2 concentration was measured by iodometric titration with KI and $Na_2S_2O_3$. To avoid its interference during COD measurements, the residual H_2O_2 was quenched using MnO_2. In all cases, the average values of the measurements are reported.

2.3. Experimental set-up

Electrochemical experiments were performed using the energy supplied by a solar panel (SOLAREX, ATERSA Inc, Spain). Table 2 shows its main characteristics. The applied potential difference (ΔE_{Cell}) between the cathode and the anode was adjusted using a voltage regulator. The electrical charge was integrated from tabular data (current *vs.* time), recorded manually from a voltage regulator display.

The SPEF experiments were conducted in a cylindrical quartz cell with 100-mL working volume. It contained two vertical electrodes,

Table 2
Photovoltaic plant main characteristics.

Module manufacturer	SOLAREX
Module model	SX-55
PV cell technology	polycrystalline silicon
Module efficiency at STC (%)	11.73
Total power at STC (P_{max}, kW)	0.055
Voltage at P_{max} (V_{mp}, V)	16.5
Current at P_{max} (I_{mp}, A)	3.33
Guaranteed minimum P_{max} (kW)	0.050
Short-circuit current (I_{sc})	3.69
Open-circuit voltage (V_{oc}, V)	20.6
Nominal Operating Cell Temperature (NOCT, °C)	47 ± 2
Total module area (m^2)	0.5184
Tracking system	Fixed
Installation	Ground
Orientation of the PV system	the tilt angle is 21.2° oriented due north
Number of cells	36 polycrystalline silicon solar cells

connected in a monopolar arrangement to power source (BK-Precision 0–30 V, 0–5 A), operating in galvanostatic mode. The electrode materials were Si/BDD (anode, dimensions: 15 × 50 × 5 mm) and titanium (cathode, dimensions: 20 × 50 × 10 mm), purchased from Fraunhofer (USA). In all experiments, the solution was stirred mechanically (240 rpm) to ensure its homogenization and reactants transport towards/from the electrodes surfaces. The sun was the UV radiation source. The SPEF trials started from noon and were running in sunny and clear days during the summer of 2016, in the EAFIT University (Medellín-Colombia). The average solar UV irradiation intensity, between 300 and 400 nm, was in the range of 20–35 W m^{-2}, as determined with a Delta OHM HD2102.1 photo-radiometer. The global irradiation intensity was in the range of 732–748 W m^{-2}, as measured with a Vantage Pro2 Davis Instruments 6162. Each experiment was performed during a period of 15 min. Fig. 1 shows the schematic of the solar – driven EO cell.

2.4. Experimental design and statistical analysis

The influence of operational parameters such as: pH, Fe^{2+} concentration, conductivity (ơ) and current density (j) on SPEF processes efficiency was investigated by means of three-level Box–Behnken experimental Design (BBD). It included 29 tests with two replicates per run and five centered experiments. The experiments were randomized using Statgraphics Centurion XVI software. Statistical analysis and modeling of the response variables (*v.g.*, the decolorization percentage (%DC), the COD reduction percentage (%DCOD), and the specific energy consumption per unit volume (E_C)) were performed with analysis of variance (ANOVA), Pareto charts and response surface modeling (RSM). RSM allows: (i) to evaluate the possible relationships between experimental factors and response variables, according to one or more selected criteria; and (ii) to find out the optimal operational conditions. Details of this methodology have been reported elsewhere [3,5,25]. The ranges of each parameter were selected basing on the preliminary experimental results (not shown here) and the data from the literature [16,17], as follows: pH = 3–6.7, Fe^{2+} concentration = 0–0.3 mM, ơ = 4560–6440 μS/cm and j = 10–50 mA/cm^2. The other variables, such as initial pollutant concentration and wastewater turbidity, were kept from the natural conditions of the TWW sample. Reaction runs were performed during 15 min, time needed to accomplished permissible discharge limits, defined by Colombian legislation. It was established on the basis of preliminary tests (not included here).

The response variables were calculated as follows:

$$\%\mathrm{DCOD} = \frac{\mathrm{COD}_0 - \mathrm{COD}_t}{\mathrm{COD}_0} \times 100 \quad (5)$$

where COD_0 and COD_t are the COD concentration before electrolysis and after electrolysis time t, respectively.

$$\%\mathrm{DC} = \frac{Ab_0 - Ab_t}{Ab_0} \times 100 \quad (6)$$

where Ab_0 and Ab_t are the absorbances before electrolysis and after electrolysis time t, respectively, at the maximum visible wavelength

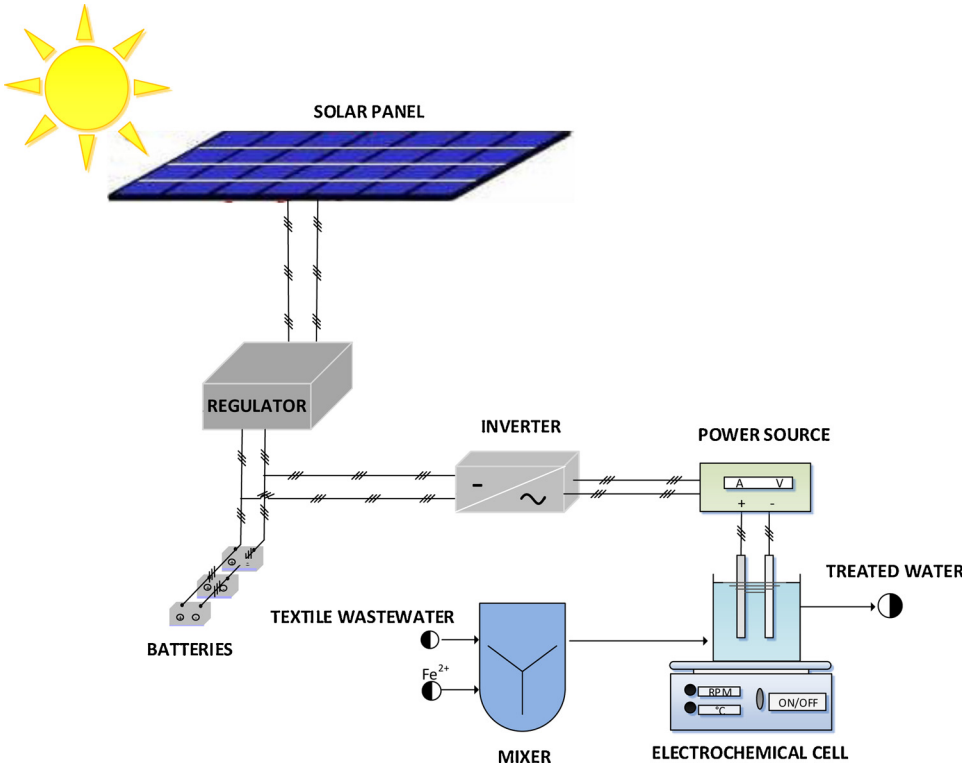

Fig. 1. Schematic of the SPEF process using Si/BDD (anode) and titanium (cathode) electrodes.

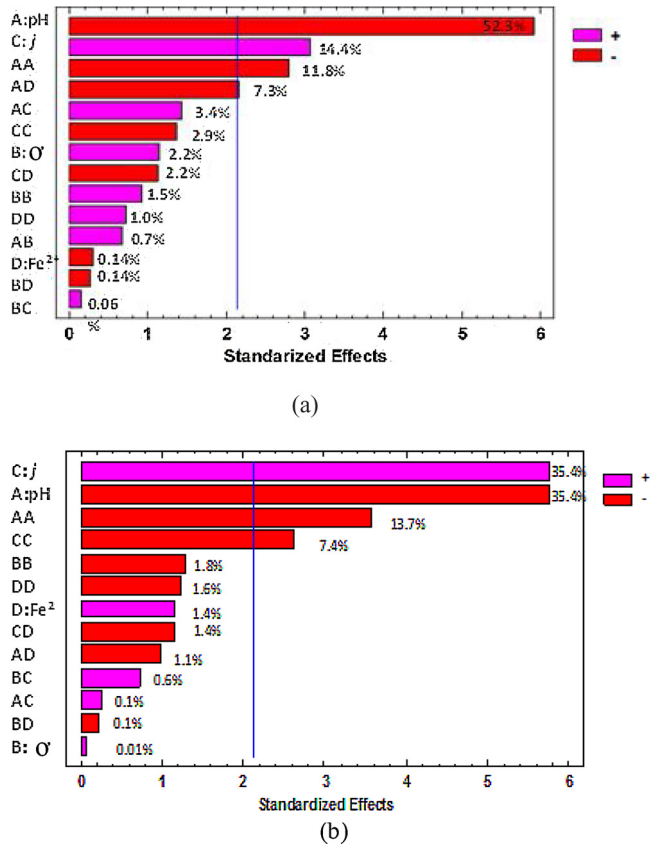

Fig. 2. Pareto diagram for (a) %DC and (b) %DCOD.

(λ_{max} = 680 nm).

$$Ec\left(\frac{kWh}{m^3}\right) = \frac{E_{cell} \times I \times t}{V_S} \quad (7)$$

where E_{cell} is the average potential difference of the cell (V), I is the average applied current (A), t is the electrolysis time (h), *Vs* is the solution volume (m^3).

$$OC = a\times Ec + b\times C_{electrolyte} + c\times C_{Fe^{2+}} + d\times C_{H_2SO_4} \quad (8)$$

The operating cost (OC, USD/m^3), where E_C is the energy consumption, $C_{electrolyte}$ is the amount of electrolyte consumed (kg/m^3), $C_{H_2SO_4}$ is the amount of H_2SO_4 consumed (kg/m^3) and $C_{Fe}{}^{2+}$ is the amount of Fe^{2+} consumed (kg/m^3). The letters a, b, c and d are unit prices for the Colombian market in October 2016, as follows: (a) electrical energy price = 0.18 USD/kWh, (b) electrolyte NaCl price = 0.3 USD/kg, (c) $FeSO_4{\cdot}7H_2O$ price = 0.45 USD/kg and (d) H_2SO_4 price = 0.6 USD/kg.

For the RSM, the experimental results were adjusted to a second-order multi-variable polynomial model, Eq. (9), using Statgraphics Centurion XVI Software.

$$Y_i = \beta_0 + \sum_1^3 \beta_i x_i + \sum_1^3 \beta_{ii} x_{ii}^2 + \sum_1^3 \sum_1^3 \beta_{ij} x_i x_j \quad (9)$$

where: β_o, β_i, β_{ii}, β_{ij} are the regression coefficients for: the intercept, lineal, square and interaction terms, respectively; Y_i is the response variable and x_i and x_j are independent variables (parameters). The quality of the models and their prediction capacity were judged from the variation coefficient of determination (R^2).

3. Results and discussion

3.1. Effect of operating parameters and optimization

Regression analysis was performed to fit the responses functions. The details of the experimental design together with the experimental data are given in the Supplementary material. The experimental results were adjusted to Eq. (9) obtaining the following expressions:

$$\%DC = 166.17 + 9.19 \times pH - 0.041 \times o' + 0.5928 \times j + 102.53 \times Fe - 2.60 \times pH^2 + 0.0016 \times pH \times o' - 0.31 \times pH \times j - 15.77 \times pH \times Fe + 3.32E^{-6} \times o^2 - 6.65E^{-5} \times o' \times j - 0.0038 \times pH \times Fe - 0.043 \times j^2 - 1.51 \times j \times Fe + 25.23 \times Fe^2 \quad (10)$$

$$\%DCOD = -241.76 + 37.57 \times pH + 0.0683 \times o' + 3.34 \times j + 159.1 \times Fe - 4.76 \times pH^2 + 0.0811 \times pH \times j - 10.36 \times pH \times Fe - 6.68E^{-6} \times o^2 + 4.52E^{-4} \times o' \times j - 4.43E^{-3} \times o' \times Fe - 0.1203 \times j^2 - 2.25 \times j \times Fe - 62.78 \times Fe^2 \quad (11)$$

$$OC\left(\frac{USD}{m^3}\right) = -3.0378 + 0.1070 \times pH + 0.001 \times o' + 0.4445 \times j + 0.50 \times Fe - 0.0136 \times pH^2 - 8.71E^{-8} \times o^2 + 2.08E^{-8} \times j^2 + 4.17E^{-6} \times j \times Fe - 0.556 \times Fe^2 \quad (12)$$

ANOVA was used to determine the significant main and interaction effects of factors influencing the %DC and %DCOD. It consists of classifying and cross-classifying statistical results, decomposing the contribution of each parameter and their double-interactions in the variance of each response variable. The *p*-values were used to identify experimental parameters that present significant statistical influence on a particular response. If a *p*-value is lower than 0.05, it is statistically significant with the 95% confidence level [5,27]. According to ANOVA results (presented in the Supplementary material), pH, *j* as well as the following double-interactions and quadratic terms: (i) for %DC: pH-pH, pH-Fe^{2+}; and (ii) for %DCOD: pH-pH, *j*-*j*, yielded *p*-values < 0.05, implying their statistically significant effects. In contrast, the effect of Fe^{2+} concentration was not statistically significant in the analyzed experimental range. This probably due to the minor changes in effluent alkalinity proportioned by OH^- production (Eq. (2)). The quality of each of the adjusted models was analyzed based on the coefficient of determination (R^2). The closer the R^2 value to unity is, more accurate the response predicted by the model could be. The R^2 values were found to be 0.928 and 0.948, for %DC and %DCOD, respectively; being in good agreement with the adjusted ones (R^2_{adj}).

The Pareto analysis (Fig. 2) was used to identify factors presenting the greatest cumulative effect on response variables. The result of this analysis can be presented as a series of bars, arranged in descending order of lengths from left to right, where length reflects the frequency or the impact of each factor and/or interaction. Therefore, the factors represented by the longest bars are relatively more significant. Here, the Pareto analysis was also used to determine the percentage effect (PE) of each factor according to Eq. (13), as follows:

$$PE_i = \left[\frac{b_i^2}{\Sigma b_i^2}\right] \times 100 (i \neq 0) \quad (13)$$

where b_i represents the value of each i factor. Statistically important factors link to all these that values overpass the inner vertical line (Fig. 2), which corresponds to the *t* value in the *t-student* distribution with a 95% confidence for 28° of freedom. Therefore, it is possible to say that following factors affect significantly the response variables:

i. **For the%DC**: pH, *j* and pH-pH, pH-Fe^{2+} interactions were identified as the main parameters affecting the%DC. Moreover, it is

directly proportional (+) to the *j* and inversely proportional (−) to pH, pH-pH and pH-Fe^{2+} interactions. One can see that pH (3– 6.7) and *j* (10–50 mA) present the strongest effect on %DC. In fact, due to the high conductivity of the treated solution (high salt content), active chlorine species can be expected to play a significant role during the EO reaction. Such activity strongly depends on the solution pH: (i) at pH of *ca.* 4, Cl_3^- is formed in very low concentration; (ii) at a pH ≈ 3, $Cl_{2,aq}$ is the predominant species; and (iii) at pH in the range of 3–8 and at pH > 8.0, HClO and ClO^-, respectively, are mainly present. Thus, Cl^- mediated oxidation of TWW is expected to be faster under acidic than that in alkaline media. This due to higher standard potential of $Cl_{2,aq}$ (E° = 1.36 V/SHE) and HClO (E° = 1.49 V/SHE) comparing to that of ClO^- (E° = 0.89 V/SHE) [6]. On the other hand, decolorization enhancement at high *j* values can be accounted by an increase in rate of reaction (1), causing higher amount of $\cdot OH_{ads}$ that in turn can yield high quantity of H_2O_2 needed in the Fenton reaction, Eq. (2). The intensified production of both type of hydroxyl radicals, $\cdot OH_{ads}$ and ·OH, accelerates the oxidation of the parent molecules and their colored products that absorb at analogous λ_{max}. Notice that Cruz-González et al. [23] reported similar results.

ii. **For the%DCOD:** *j*, pH, pH-pH and *j-j* interactions are the most important factors affecting COD degradation efficiency. %DCOD is directly proportional (+) to *j* and inversely proportional (−) to pH, pH-pH and *j-j* interactions. Moreover, *j* and pH appear to be the most significant factors. In fact, they both control the rate of oxidizing species generation. The Fe^{2+} added to the solution strongly increases the oxidation power of the electrogenerated H_2O_2. An advantage of the electro-Fenton process is the catalytic behavior of the Fe^{3+}/Fe^{2+} system: Fe^{2+} is oxidized by H_2O_2 in Fenton's reaction, Eq. (2), giving rise to ·OH radicals and Fe^{3+}; whereas Fe^{3+}, obtained or initially added to the solution, is continuously reduced to Fe^{2+}. Organic matter is then oxidized by the combined action of ·OH produced at the anode from reaction (1) and in the homogeneous medium from Fenton's reaction (2), reaching high degradation percentage in a short time. Notice that ·OH radicals can be produced at higher rate by the simultaneous reactions (2) and (3). In addition, complexes of Fe^{3+} with carboxylic acids (*v.g.,* oxalic acid), generated from the initial pollutants, can be quickly photo-decomposed into CO_2, enhancing the degradation rate of organic matter and dyes [28].

In order to determine the integrated effect of *j* and pH on the response variables, three-dimensional response surface plots were used (Fig. 3). Notice that %DC and %DCOD increased with an increase in *j* whereas decreases with an increase in pH. The maximum %DC removal efficiency was achieved in the ranges of 30 < *j* < 50 mA/cm^2 and a 3 < pH < 4 (Fig. 3a). On the other hand, COD removal percentage improved with an increase in applied current density, Fig. 3(b). This can be expected due to the improvement in oxidant production. However, higher values of applied *j* mean higher applied voltage in the electrochemical system as well as higher OC (Fig. 3c). From these results, the following optimal operational conditions for the SPEF process were determined: pH = 4, *j* = 40 mA/cm^2, σ = 5768 μS/cm and Fe^{2+} = 0.3 mM. Table 1 summarizes its experimental verification, in an independent run, with the characteristics of treated wastewater. One can see that the global efficiencies are quite high. Notice that it is possible to achieve total discoloration and high mineralization (see also additional data in Table 1 for comparison). Moreover, the final effluent achieved the last environmental Colombian regulation.

3.2. Kinetic studies

At the optimized SPEF conditions, a kinetic analysis was developed. Color, COD and TOC were monitored as a function of time (Fig. 4). For all cases, removal efficiencies increased with the increase in electrolysis

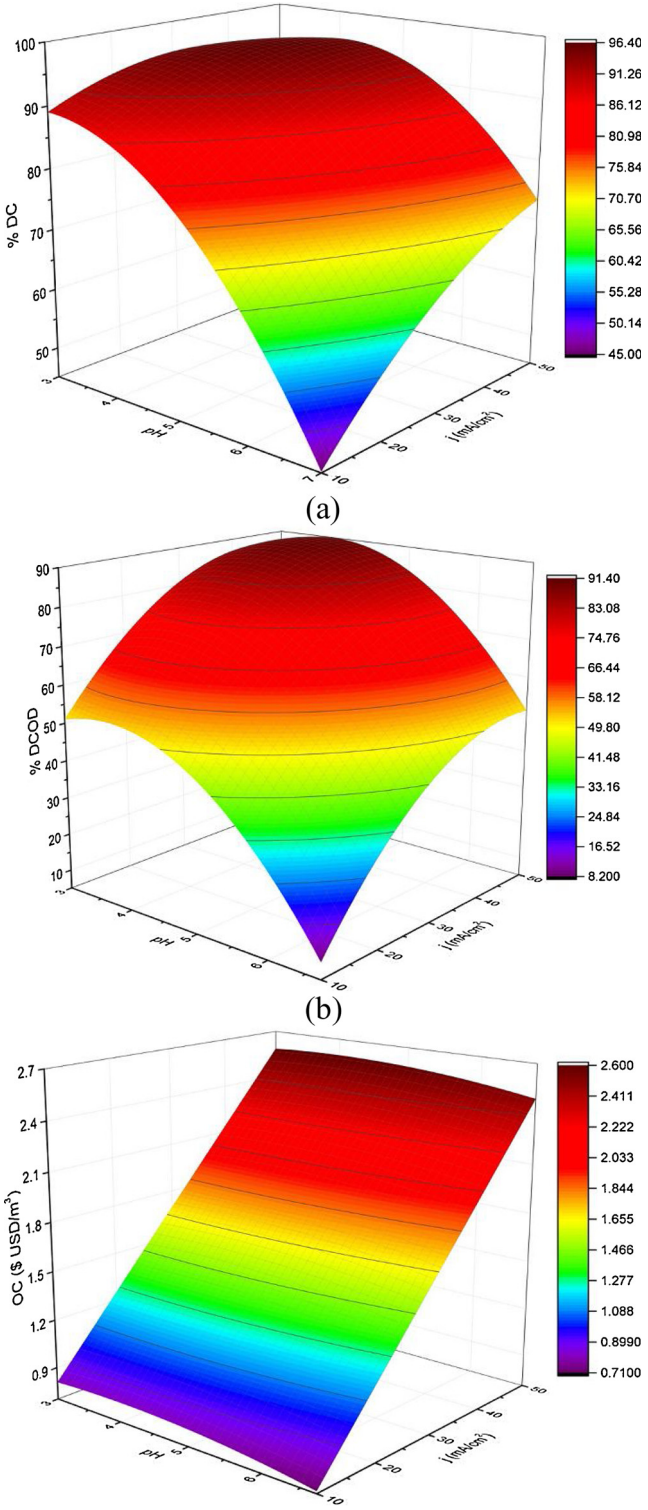

Fig. 3. Three-dimensional surface response plots for the interactive effect of ***j*** and pH on: (a) %DC, (b) %DCOD and (c) OC. Electrolysis time = 15 min, Fe^{2+} concentration = 0.3 mM, σ = 5768 μS/cm and A/V = 7.5 m^{-1}.

time. A very rapid color drop was observed during the first three minutes of treatment, decreasing its degradation rate after that time. The COD and TOC degradation reached *ca.* 90% and 80%, respectively, after 15 min of treatment. Thus, the COD concentration was reduced below the discharge limit according to Colombian regulation.

The obtained results are in agreement with previously reported ones in open literature. Garcia-Segura et al. [11] stated an almost total

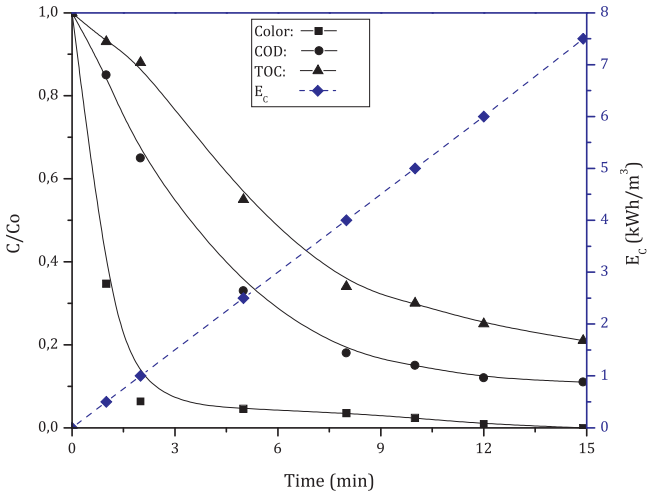

Fig. 4. Evolution of color, COD, TOC and E_c *vs.* electrolysis time. Experimental conditions: pH = 4, j = 40 mA/cm^2, σ = 5768 μS/cm, A/V = 7.5 m^{-1}, Fe^{2+} = 0.3 mM.

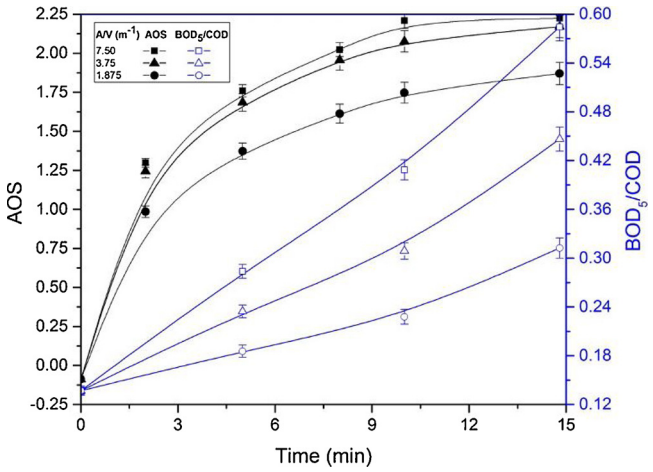

Fig. 5. Evolution of chemical and biological wastewater characteristics of treated effluent during the SPEF process. Experimental conditions: pH = 4, j = 40 mA/cm^2, σ = 5768 μS/cm, Fe^{2+} = 0.3 mM.

mineralization (*i.e.*, 97% TOC abatement) of 200 mg/L dye solution of Acid Orange 7, Disperse Blue 71 or Acid Red 151 using PEF (100 mL, 0.5 mM Fe^{2+}, pH = 3.0 and a 6 W UVA light at 200 mA), much higher than 85% of TOC reduction accomplished by EF. On the other hand, Khataee et al. [12,29] evaluated EF and PEF processes for the direct decolorization of Red 23, using a flow tank reactor equipped with Pt (anode) and a carbon nanotube (CNT)-PTFE (cathode), fed with pure O_2 and connected to a cylindrical Pyrex photoreactor with an internal 15W UVC lamp. The electrolysis of 30 mg/L dye solution (2 dm^3, 0.05 mM Fe^{3+}, at pH = 3.0, 300 mA) yielded 66 and 94% of decolorization using EF and PEF, respectively. Both groups achieved higher mineralization degrees using PEF due to much faster photolysis of Fe(III)-carboxylate complexes than that reached by both heterogeneous BDD(·OH) and homogeneous ·OH processes, during EF. Also, Salazar et al. [30] settled the SPEF process, with Fe^{2+}, as an emerging EAOP, able to become competitive as wastewater remediation technology, stressing as its advantage the capacity of natural UV radiation to oxidize dissolved contaminants. The effect of sunlight and Fe^{2+} was demonstrated during the treatment of an industrial pollutant containing anthraquinonic dyes. The complete decolorization and mineralization of solutions was achieved within relatively short time (v.g., 30 min) [32]. Moreover, the operational costs of the integrated SPEF process reached 1.56 USD/m^3, relatively realistic and modest value which agrees with some others reported in the literature (OC ranges from 0.50 USD/m^3 to 14.50 USD/m^3) [4,10,30–32].

Valuable additional information, regarding the reaction progress during the SPEF wastewater treatment, can be obtained analyzing the Average Oxidation State (AOS) of the treated sample. AOS can be calculated as follows [33]:

$$AOS = 4 - 1.5 \times \frac{COD}{TOC} \quad (14)$$

where TOC and COD are expressed in mg of C/L and mg of O_2/L, respectively. The AOS can take a value between +4, for the most oxidized state of carbon (CO_2), and −4, for the most reduced state of carbon (CH_4). One can see (Fig. 5) that, after 15 min of SPEF treatment, AOS rises gradually from −0.0875 up to 2.24 (for A/V = 7.5 m^{-1}). Thus, it can be inferred that the SPEF effluent contains highly oxidized compound. This characteristic usually improves the wastewater biodegradability. In fact, the effluent BOD_5/COD ratio increased from 0.2165 up to 0.5845, confirming its biocompatible characteristics.

3.3. Effect of A/V ratio on the degradation efficiency

The electrodes' effective surface area (A/V ratio) is an important parameter for electrochemical activity in large-scale application. To evaluate the influence of the A/V ratio on SPEF degradation efficiency, it was changed by varying the anode area (A, m^2), keeping the wastewater volume (m^3) constant. It was found that there is a positive relationship between the amount of ·OH generated and the A/V ratio of the BDD electrode. The evolution of AOS and BOD_5/COD ratio, realized at optimized conditions and three different A/V ratios, is presented in Fig. 5. Notice that AOS rises gradually from −0.0875 to 1.8 and 2.1 while BOD_5/COD ratio increases from 0.2165 to 0.3125 and 0.4465 for A/V = 1.875 m^{-1} and 3.75 m^{-1}, respectively. Additionally, the variations of TOC and E_c *vs.* time is presented in Fig. 6. It can be observed that both TOC degradation and E_c increased with an increase in A/V ratio. Notice that very similar results of AOS (Fig. 5) and TOC degradation (Fig. 6) were obtained after 15 min electrolysis using either A/V ratio equals to 7.5 m^{-1} or 3.75 m^{-1}. However, A/V ratio equals to 3.75 m^{-1} implies not only lower energy consumption but also let to the last environmental Colombian regulation with regard to BOD_5 content (Fig. 5). Therefore, the A/V ratio equaled to 3.75 m^{-1} was chosen as the most suitable one.

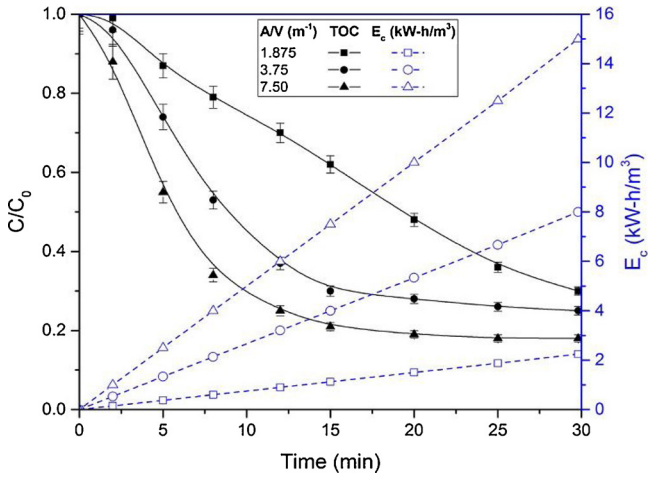

Fig. 6. Effect of the variation of the A/V ratio on the TOC degradation efficiency and E_c *vs.* electrolysis time. Experimental conditions: pH = 4, j = 40 mA/cm^2, σ = 5768 μS/cm, Fe^{2+} = 0.3 mM.

4. Conclusions

A Solar-Photo-Electro-Fenton process was applied as alternative for the treatment of industrial textile wastewater. At optimum operational conditions (pH = 4, $j = 40\,mA/cm^2$, $\sigma = 5768\,\mu S/cm$ and $Fe^{2+} = 0.3\,mM$) the solar-driven process let to obtain total discoloration, COD reduction of 83% and TOC mineralization of 70% after 15 min of electrolysis. The solar-driven process yielded a highly oxidized (AOS = 2.24) and biocompatible ($BOD_5/COD > 0.4$) effluent. Additionally, the most suitable effective surface area of the electrodes (A/V ratio) was equivalent to $3.75\,m^{-1}$, important considering process scale-up. The operational costs were estimated at 1.56 USD/m^3, demonstrating SPEF as an efficient and economical alternative for the treatment of industrial textile wastewater effluents.

Acknowledgments

The authors thank to the "Dirección de Investigación" de la Universidad EAFIT, Medellín, Colombia for the financial support of this research. The staff of the "Laboratorio de Ingeniería de Procesos" is also recognized for their participation.

Appendix A. Supplementary data

Supplementary data associated with this article can be found, in the online version, at https://doi.org/10.1016/j.jwpe.2018.05.007.

References

[1] J.M. Aquino, R.C. Rocha-filho, L.A.M. Ruotolo, N. Bocchi, S.R. Biaggio, Electrochemical degradation of a real textile wastewater using β-PbO_2 and DSA anodes, Chem. Eng. J. 251 (2014) 138–145.
[2] H. Wu, S. Wang, Impacts of operating parameters on oxidation–reduction potential and pretreatment efficacy in the pretreatment of printing and dyeing wastewater by Fenton process, J. Hazard. Mater. 243 (2012) 86–94.
[3] E. GilPavas, C.M. Gómez, J.M. Rynkowski, I. Dobrosz-Gómez, M.Á. Gómez-García, Decolorization and mineralization of yellow 5 (E102) by UV/Fe^{2+}/H_2O_2 process. Optimization of the operational conditions by response surface methodology, Comptes Rendus Chimie 18 (2015) 1152–1160.
[4] E. GilPavas, I. Dobrosz-Gómez, M.Á. Gómez-García, Coagulation-flocculation sequential with Fenton or Photo-Fenton processes as an alternative for the industrial textile wastewater treatment, J. Environ. Manage. 191 (2017) 189–197.
[5] E. GilPavas, J. Medina, I. Dobrosz-Gómez, M.Á. Gómez-García, E. GilPavas, I. Dobrosz-Gómez, M.Á. Gómez-García, Statistical optimization of industrial textile wastewater treatment by electrochemical methods, J. Appl. Electrochem. 44 (2014) 1421–1430.
[6] R.E. Palma-Goyes, J. Vazquez-Arenas, R.A. Torres-Palma, C. Ostos, F. Ferraro, I. González, The abatement of indigo carmine using active chlorine electro-generated on ternary Sb_2O_5-doped Ti/RuO_2-ZrO_2 anodes in a filter-press FM01-LC reactor, Electrochim. Acta 174 (2015) 735–744.
[7] F. Montilla, P.A. Michaud, E. Morallón, J.L. Vázquez, Ch. Comninellis, Electrochemical oxidation of benzoic acid at boron-doped diamond electrodes, Electrochim. Acta 47 (2002) 3509–3513.
[8] A. Altin, An alternative type of photoelectroFenton process for the treatment of landfill leachate, Sep. Purif. Technol. 61 (3) (2008) 391–397.
[9] C.A. Martínez-Huitle, E. Brillas, Decontamination of wastewaters containing synthetic organic dyes by electrochemical methods: a general review, Appl. Catal. B: Environ. 87 (2009) 105–145.
[10] C.A. Martínez-Huitle, E. Brillas, Decontamination of wastewaters containing synthetic organic dyes by electrochemical methods. An updated review, Appl. Catal. B: Environ. 166–167 (2015) 603–643.
[11] S. Garcia-Segura, A. El-Ghenymy, F. Centellas, R.M. Rodríguez, C. Arias, J.A. Garrido, P.L. Cabot, E. Brillas, Comparative degradation of the diazo dye Direct Yellow 4 by electro-Fenton, photoelectro-Fenton and photo-assisted electro-Fenton, J. Electroanal. Chem. 681 (2012) 36–43.
[12] A. Khataee, A. Khataee, M. Fathinia, B. Vahid, S.W. Joo, Kinetic modeling of photoassisted-electrochemical process for degradation of an azo dye using boron-doped diamond anode and cathode with carbon nanotubes, J. Ind. Eng. Chem. 19 (6) (2013) 1890–1894.
[13] Y. Hang, M. Qu, F. Zhao, Economic and environmental life cycle analysis of solar hot water systems in the United States, Energy Build. 45 (2012) 181–188.
[14] T. Muneer, S. Maubleu, M. Asif, Prospects of solar water heating for textile industry in Pakistan, Renew. Sustain. Energy Rev. 10 (1) (2006) 1–23.
[15] D. Valero, J.M. Ortiz, E. Expósito, V. Montiel, A. Aldaz, Electrocoagulation of a synthetic textile effluent powered by photovoltaic energy without batteries: direct connection behavior, Sol. Energy Mater. Sol. Cells 92 (2008) 291–297.
[16] B. Parida, S. Iniyan, R. Goic, A review of solar photovoltaic technologies, Renew. Sustain. Energy Rev. 15 (3) (2011) 1625–1636.
[17] R.A. Agathokleous, S.A. Kalogirou, Double skin facades (DSF) and building integrated photovoltaics (BIPV): a review of configurations and heat transfer characteristics, Renew. Energy 89 (2016) 743–756.
[18] A. Cabrera-Tobar, E. Bullich-Massagué, M. Aragüés-Peñalba, O. Gomis-Bellmunt, Topologies for large scale photovoltaic power plants, Renew. Sustain. Energy Rev. 59 (2016) 309–319.
[19] E. Alvarez-Guerra, A. Dominguez-Ramos, A. Irabien, Design of the Photovoltaic Solar Electro-Oxidation (PSEO) process for wastewater treatment, Chem. Eng. Res. and Des. 89 (2011) 2679–2685.
[20] H. Zhang, X. Ran, X. Wu, D. Zhang, Evaluation of electro-oxidation of biologically treated landfill leachate using response surface methodology, J. Hazard. Mater. 188 (1–3) (2011) 261–268.
[21] A. El-Ghenymy, S. Garcia-Segura, R.M. Rodríguez, E. Brillas, M. El Begranib, B. Abdelouahid, Optimization of the electro-Fenton and solar photoelectro-Fenton treatments of sulfanilic acid solutions using a pre-pilot flow plant by response surface methodology, J. Hazard. Mater. 221–222 (2012) 288–297.
[22] Z. Zhang, H. Zheng, Optimization for decolorization of azo dye acid green 20 by ultrasound and H_2O_2 using response surface methodology, J. Hazard. Mater. 172 (2–3) (2009) 1388–1393.
[23] K. Cruz-González, O. Torres-Lopez, A.M. García-León, E. Brillas, A. Hernández-Ramírez, J.M. Peralta-Hernández, Optimization of electro-Fenton/BDD process for decolorization of a model azo dye wastewater by means of response surface methodology, Desalination 286 (2012) 63–68.
[24] APHA, Standard Methods for the Examination of Water and Wastewater, 22a ed., American Public Health Association, Washington, 2012.
[25] S.L.C. Ferreira, R.E. Bruns, H.S. Ferreira, G.D. Matos, J.M. David, G.C. Brandao, E.G.P. Da Silva, L.A. Portugal, P.S. Dos Reis, Box-Behnken design: an alternative for the optimization of analytical methods, Anal. Chim. Acta 597 (2007) 179–186.
[26] M. Lapertot, S. Ebrahimi, S. Dazio, A. Rubinelli, C. Pulgarin, Photo-Fenton and biological integrated process for degradation of a mixture of pesticides, J. Photochem. Photobiol. A: Chem. 186 (2007) 34–40.
[27] D.C. Montgomery, Design and Analysis of Experiments, 8th edition, Wiley, New Jersey, USA, 2010.
[28] S. Garcia-Segura, E. Brillas, Combustion of textile monoazo, diazo and triazo dyes by solarphotoelectro-Fenton: decolorization kinetics and degradation routes, Appl. Catal. B: Environ. 181 (2016) 681–691.
[29] A.R. Khataee, B. Vahid, B. Behjati, M. Safarpour, Treatment of a dye solution using photoelectro-Fenton process on the cathode containing carbon nanotubes under recirculation mode: investigation of operational parameters and artificial neural network modeling, Environ. Progr. Sustain. Energy 32 (2013) 557–563.
[30] R. Salazar, E. Brillas, I. Sirés, Finding the best Fe^{2+}/Cu^{2+} combination for the solar photoelectro-Fenton treatment of simulated wastewater containing the industrial textile dye Disperse Blue 3, Appl. Catal. B Environ. 115–116 (115) (2012) 107—116.
[31] M. Kobya, E. Gengec, E. Demirbas, Operating parameters and costs assessments of a real dyehousewastewater effluent treated by a continuous electrocoagulation process, Chem. Eng. Process: Process Intensification 101 (2016) 87–100.
[32] P.A. Soares, R. Souza, J. Soler, T.F. Silva, S. Guelli, R.A.R. Boaventura, V.J.P. Vilar, Remediation of a synthetic textile wastewater from polyester-cotton dyeing combining biological and photochemical oxidation processes, Sep. Purif. Technol. 172 (2017) 450–462.
[33] F. Vogel, J. Harf, A. Hug, P.R.V. Rohr, The mean oxidation number of carbon (MOC) a useful concept for describing oxidation processes, Water Res. 34 (2000) 2689–2702.